IEEE Access
Multidisciplinary | Rapid Review | Open Access Journal

Received October 28, 2020, accepted November 2, 2020, date of publication November 6, 2020, date of current version November 24, 2020.

Digital Object Identifier 10.1109/ACCESS.2020.3036403

Theoretical and Experimental Study of Ultrasonic Vibration-Assisted Laser Polishing 304 Stainless Steel

DI KANG, PING ZOU, HAO WU, WENJIE WANG, AND JILIN XU
School of Mechanical Engineering and Automation, Northeastern University at Shenyang, Shenyang 110819, China
Corresponding author: Ping Zou (pzou@mail.neu.edu.cn)

This work was supported in part by the National Natural Science Foundation of China under Grant 51875097.

ABSTRACT With the increasing requirements for the surface quality of the workpiece, many kinds of hybrid manufacturing have developed recently. Ultrasonic vibration-assisted laser polishing (UVLP) is a new hybrid manufacturing method. Different from the traditional method of applying ultrasonic vibration on the workpiece, this article applies ultrasonic vibration on the lens. Besides, the thermal mechanisms of the 304 stainless steel polished by traditional laser polishing (TLP) and UVLP were analyzed to reveal the influence of ultrasonic vibration on the polishing effect. The ultrasonic vibration lens transforms the laser polishing into an intermittent polishing process, which affects the laser energy density and the quality of the polished surface. This research was focused on the experimental analysis of the surface morphology and surface roughness of the 304 stainless steel that was processed by UVLP, and compared with TLP. And the effects of laser power, scanning speed, focus offset, and amplitude on the quality of the polished surface were obtained. The preferred process parameters of UVLP 304 stainless steel were obtained by the range analysis and variance analysis of the orthogonal experiment. Experimental results have shown that UVLP can reduce the surface roughness of 304 stainless steel from 2.777 μm to 0.512 μm at most. Thermal mechanism analysis results were verified by experimental results. Choosing appropriate processing parameters can effectively improve the quality of the polished surface, making the processing effect of UVLP significantly better than TLP.

INDEX TERMS Hybrid manufacturing, ultrasonic vibration-assisted laser polishing, traditional laser polishing, thermal mechanism analysis, orthogonal experiment.

NOMENCLATURE

ABBREVIATION

UVLP	Ultrasonic vibration-assisted laser polishing
TLP	Traditional laser polishing
PFAM	Powder feed metal additive manufacturing
SSM	Shallow surface melting
SOM	Surface over melt

SYMBOL

ρ	Density (g·cm^{-3})
C	Specific heat (J·g^{-1}·K^{-1})
T	Temperature (K)
t	Laser irradiation time (s)
K	Heat conductivity of the material (W·cm^{-1}·K^{-1})
Q	Calorific value of the material per unit volume per unit time (J)
α	Thermal diffusivity of the material (cm^2·s^{-1})
A_b	Absorptivity of the material to the laser
I	Laser energy density (W·cm^{-2})
$erfc$	Error function
$ierfc$	Integral of the error function
ρ (T)	Metal resistivity
R_i	Radius of incident laser waist (cm)
R_0	Radius of output laser waist (cm)
z_i	Distance between the waist of incident laser and lens (cm)
F_a	Focal length (cm)
f_F	Dimensional parameters
z_0	Distance between the waist of output laser and lens (cm)

The associate editor coordinating the review of this manuscript and approving it for publication was Agustin Leobardo Herrera-May.

$R_{(z)}$	Spot radius irradiated on the 304 stainless steel workpiece surface (cm)
P	Laser power (W)
A	Ultrasonic vibration amplitude (μm)
Z_l	Distance between the waist of incident laser and polished surface (cm)
λ	Laser wavelength (nm)
f	Ultrasonic frequency (kHz)
z'	Distance from polished surface to the waist of the output laser (cm)
$R'_{(z)}$	Radius of the beam waist (cm)
V	Scanning speed (m/min)
z	Focus offset (cm)
Sa	Surface roughness (μm)
T_s	Solidus temperature (K)
T_l	Liquidus temperature (K)
T_m	Melting point (K)
T_b	Boiling point (K)
i	Number of factors
j	Number of levels
K	Average value
R	Range value
k_j	Number of levels on any column
SS_i	Sum of square deviation for each factor
SS_T	Total sum of square deviation
SS_E	Sum of square deviation for experimental error
MS_i	Mean-square deviation of each factor
MS_E	Mean-square deviation experimental error
DF_i	Degree of freedom for each factor
DF_E	Degree of freedom for experimental error
F_i	F-value of each factor

I. INTRODUCTION

With the development of advanced technologies such as aerospace and ship, the requirements for equipment performance are constantly increasing. Consequently, the surface quality of the aero-engine blade and ship propeller needs to be improved. At present, polishing is the primary final processing to reduce the surface roughness of components and remove the damaged layer that is formed by the previous process. It can eliminate the residual stress on the surface and obtain a smooth and non-damaged machined surface. Polishing accounts for about 30% of the total processing cost. In the modern manufacturing industry, commonly used polishing techniques are mechanical polishing, chemical polishing, electrochemical polishing, ultrasonic polishing, and laser polishing [1]–[4]. In recent years, laser polishing has been widely studied as a new polishing method which can effectively improve the surface quality. A focused laser beam is applied to the surface of the workpiece to melt the microlayer. The molten material is flowed by surface tension and gravity. In this way, the surface micro-bulge is reduced and the surface dimple is filled [5]–[7]. Laser polishing is a non-contact polishing method that can avoid surface orientation caused by polishing, and it is more conducive to polishing 3-D complex-shaped workpieces [8]. Moreover, laser polishing has the advantage of polishing for high hardness materials [9]–[11]. It is regarded as a new surface final processing technology, which is promising to replace the time-consuming and error-prone manual polishing [12], [13].

The theoretical modeling of laser beam machining was investigated in a few published works in the past. Ukar *et al.* [14] presented a thermal model of metallurgical transformations during laser polishing. This thermal model is very helpful for predicting the distribution of the temperature field and the thickness of the melting layer. Ning *et al.* [15] reported a high prediction accuracy and high computational efficiency physics-based predictive model to estimate the in-process temperature in powder feed metal additive manufacturing (PFAM). Laser power absorption, scanning strategy, heat transfer boundary condition, and latent heat were considered in the prediction of time-dependent thermal profiles. Kundakcıoğlu *et al.* [16] developed an adjustable finite element-based multi-physics and multi-software platform thermal model to predict the transient temperature and the molten pool geometry. Mohajerani *et al.* [17] carried out a study for the development of laser polishing models. Laser polishing is the result of several overlapping thermophysical phenomena, and the modeling of the laser polishing process remains a challenging task.

The focused laser beam is applied to the surface of the workpiece to be machined. Because of the high temperature of the laser beam, a molten pool is formed on the thin layer of the workpiece surface. Under the action of multi-direction forces such as gravity and surface tension, the molten material is relocated from peaks to valleys and re-solidified again [18]. Ramos-Grez and Bourell [19] proposed that laser polishing metal materials should be divided into two processes: shallow surface melting (SSM) and surface over melt (SOM). Yung *et al.* [20] used pulsed lasers and continuous-wave lasers to polish tool steel components respectively under different technological conditions and obtained excellent surface quality. Mai and Lim [21] studied laser polishing of 304 stainless steel and analyzed the surface morphology, reflectivity, hardness, and corrosion resistance of 304 stainless steel after polishing. Bhaduri *et al.* [22] noticed that laser polishing can reduce the surface roughness of 3-D printed components and without affecting the geometric accuracy. Obeidi *et al.* [23] also reported laser polishing the surface of 316L stainless steel components that were produced by additive manufacturing. The results have shown that the maximum decrease range of surface roughness was from 10.4 μm to 2.7 μm, and there was no significant change in microstructure and micro-hardness.

Although a great deal of work on laser polishing has been published in the past 30 years, the precision and quality of laser polishing still need to be improved. When the focused laser is irradiated to remove the metallic material locally, excessive laser incidence will cause thermal damage to the processed surface. Scholars combine ultrasonic vibration of the workpiece with laser machining to improve the quality of laser processing. Kang *et al.* [24] have shown

that ultrasonic vibration was applied to laser processing for improving the surface quality. Alavi and Harimkar [25] presented that ultrasonic vibration-assisted laser surface melting austenitic stainless steel can remove materials more effectively. Under the condition that the vibration frequency was 18 kHz and the amplitude was 20 μm, the diamond particles have a strong impact on the surface of WC-Co cemented carbide. The recombination of laser processing could make it smoother and the final roughness reached 7.6 nm [26]. Wu *et al.* [27], [28] proposed using vibrating-lens to assist laser machining of patterns and holes. Meanwhile, a theoretical model of vibrating-lens assisted laser machining process was established and proved by experiments. The ultrasonic vibration of the workpiece assisted laser processing is beneficial to the improvement of the surface quality. However, it is difficult to ensure that the large workpiece is still in the ultrasonic vibration state. Improving surface quality has been the most challenging issue in the laser polishing fields.

In this article, a creative method of ultrasonic vibration-assisted laser polishing (UVLP) is developed to improve the polished surface quality of the 304 stainless steel. Lens ultrasonic vibration makes the UVLP processing more flexible and stable. Theoretical analysis of the thermal model reveals the effect of lens ultrasonic vibration on the temperature of the molten pool, which is formed by laser polishing. The effect of each experimental factor on the polishing of 304 stainless steel is confirmed by comparative experiment and orthogonal experiment. Finally, the preferred process parameters of ultrasonic vibration-assisted laser polishing 304 stainless steel are obtained under the designed experimental setup. Compared with ultra-precision machining, the UVLP is a non-contact polishing method. It can reduce the microcracks on the processed surface and improve the machining efficiency.

II. THERMAL MECHANISM OF 304 STAINLESS STEEL POLISHED BY TLP AND UVLP

The continuous-wave laser polishing of the metal surface is mainly based on the thermal effect that is produced by the interaction between material and laser. The polishing effect is obtained by melting, evaporating, and other thermal interaction to remove the thin layer of material on the surface. Remelting polishing is the main method of laser polishing on the metal surface. Therefore, the influence of the ultrasonic vibration lens on the surface quality of laser polished 304 stainless steel is explained by studying the change of molten pool temperature.

When the laser irradiates the surface of the metal material, the laser energy is absorbed by the surface material and converted into heat. The heat generated by a heat source is diffused in the material through the heat conduction and formed a temperature field. The thermal mechanism of laser polishing 304 stainless steel with or without an ultrasonic vibration lens is shown in Fig. 1.

It is very difficult to solve the analytic solution of the partial differential equation under boundary conditions in the theoretical analysis of the laser polishing metal material. In order to reveal the nature of heat transfer and simplify the calculation, the following assumptions are made:

1) The optical and thermodynamic parameters of the material are independent of temperature.

2) The 304 stainless steel is uniform and thermophysical properties of isotropic material.

3) Thermal radiation and convection are ignored in the heat transfer process, and only the inward heat conduction on the material surface is considered.

The general form of the partial differential equation of heat conduction is [29]:

$$\rho \cdot C \cdot \frac{\partial T}{\partial t} = K \cdot \left(\frac{\partial^2 T}{\partial x^2} + \frac{\partial^2 T}{\partial y^2} + \frac{\partial^2 T}{\partial z^2} \right) + Q\,(x, y, z, t) \tag{1}$$

where ρ (g·cm^{-3}) is the density, C (J·g^{-1}·K^{-1}) is the specific heat, T (K) is the temperature, t (s) is the laser irradiation time, K (W·cm^{-1}·K^{-1}) is the heat conductivity of the material, and Q (J) is the calorific value of the material per unit volume per unit time.

Most of the laser energy is absorbed by the surface of the material, so the volume heat source can be ignored during polishing. Assuming $Q = 0$, Eq. (1) can be expressed as:

$$\frac{\partial^2 T}{\partial x^2} + \frac{\partial^2 T}{\partial y^2} + \frac{\partial^2 T}{\partial z^2} - \frac{1}{\alpha} \cdot \frac{\partial T}{\partial t} = 0 \tag{2}$$

where α (cm^2·s^{-1}) is the thermal diffusivity of the material.

When the size of the laser spot is larger than the depth of heat penetration within the laser irradiation time, it is treated as one-dimensional heat conduction. The process of continuous-wave laser polishing 304 stainless steel in this study is approximately treated as one-dimensional heat conduction perpendicular to the surface of the workpiece (Z direction, in Fig. 1). The heat conduction equation is as follows:

$$\frac{\partial^2 T}{\partial z^2} - \frac{1}{\alpha} \cdot \frac{\partial T}{\partial t} = 0 \tag{3}$$

The surface without irradiated by the laser is regarded as an adiabatic boundary, and the boundary condition is [30]:

$$A_b \cdot I = -K \cdot \frac{\partial T}{\partial z} \tag{4}$$

where A_b is the absorptivity of the material to the laser, and I is the laser energy density.

Combined with Eq. (4), Eq. (3) is solved as follows:

$$T\,(z, t) = \left(2A_b I \big/ K\right) \cdot \sqrt{\alpha t} \cdot ierfc\left(z \Big/ \sqrt{4\alpha t}\right) \tag{5}$$

where *ierfc* is the integral of the error function *erfc*, that is,

$$\begin{cases} ierfc\,(x) = \int_x^\infty erfc\,(s)ds \\ erfc\,(x) = \dfrac{2}{\sqrt{\pi}} \displaystyle\int_x^\infty e^{-s^2} ds \end{cases} \tag{6}$$

According to Eq. (5), the surface temperature of the material irradiated by laser is:

$$T\,(t) = T_0 + \left(2A_b I \big/ K\right) \sqrt{\alpha t / \pi} \tag{7}$$

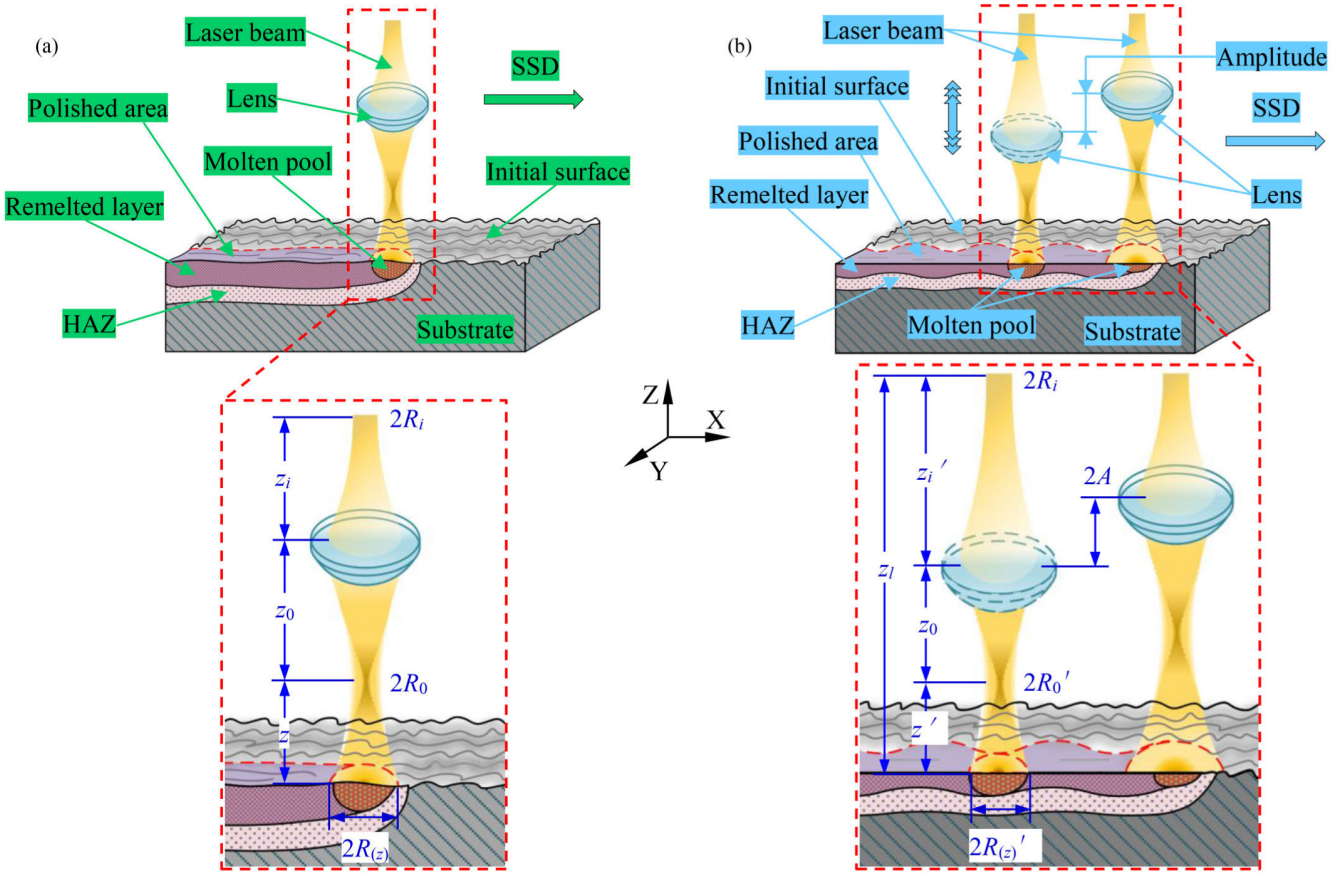

FIGURE 1. The thermal mechanism of polishing the 304 stainless steel between (a) TLP and (b) UVLP.

The heat conductivity of 304 stainless steel was measured based on laser rapid heating and computer automatic collection of multi-point temperature technology. Through the regression analysis of the curve, the calculation equation of the heat conductivity of 304 stainless steel changing with temperature is obtained [31]:

$$K = 0.03787 + 0.00024T \tag{8}$$

Metal resistivity is an important parameter contributing to laser absorption. The resistivity of the metal increases with the raise of temperature, which leads to the enhancement of the material's absorption for the laser. Theoretical values of the absorptivity of metals are obtained using the Hagen-Ruben relationship. The absorptivity for continuous-wave laser ($\lambda = 1064$ nm) is found to be [32]:

$$A_b(T) = 354.67\sqrt{\rho\,(T)} \tag{9}$$

where ρ (T) is the metal resistivity, which is an equation of temperature change. The resistivity of the 304 stainless steel varies with temperature as follows [33]:

$$\rho\,(T) = 10^{-8}\left[60 + 5\times10^{-4}\,(T)\right], \quad 273K \le T \le 1700K \tag{10}$$

The ultrasonic vibration lens mainly affects the laser energy density on the surface of the 304 stainless steel workpiece. According to the conversion principle of the Gaussian beam through a thin lens, the laser beam output after the Gaussian beam irradiates on the lens is still a Gaussian beam. The spot on the surface of the workpiece irradiated by TLP is shown in Fig. 1 (a). At the focus, the distance from the lens to the beam waist of the output Gaussian beam and the radius of the beam waist are respectively:

$$R_0 = \frac{R_i \cdot F_a}{\left[(z_i - F_a)^2 + f_F^2\right]^{1/2}} \tag{11}$$

$$z_0 = \frac{F_a \cdot \left[z_i \cdot (z_i - F_a) + f_F^2\right]}{(z_i - F_a)^2 + f_F^2} \tag{12}$$

where R_i is the radius of incident laser waist, R_0 is the radius of output laser waist, z_i is the distance between the waist of incident laser and lens, F_a is the focal length, f_F is the dimensional parameters, and z_0 is the distance between the waist of output laser and lens.

The spot radius $R_{(z)}$ irradiated on the surface of the 304 stainless steel workpiece is:

$$R_{(z)} = \frac{\sqrt{\left(\pi \cdot R_i^2 \cdot F_a^2\right)^2 + \left\{\lambda \cdot z \cdot \left[(z_i - F_a)^2 + f_F^2\right]\right\}^2}}{\pi \cdot R_i \cdot F_a \cdot \sqrt{(z_i - F_a)^2 + f_F^2}} \tag{13}$$

Based on the Gaussian heat flux, the energy density in the spot can be expressed as [34]:

$$I(z) = \frac{2P}{\pi \cdot R_{(z)}^2} = \frac{2P \cdot \pi \cdot R_i^2 \cdot F_a^2 \cdot \left[(z_i - F_a)^2 + f_F^2\right]}{\left(\pi \cdot R_i^2 \cdot F_a^2\right)^2 + \lambda^2 \cdot z^2 \cdot \left[(z_i - F_a)^2 + f_F^2\right]^2} \tag{14}$$

where P is the laser power.

The spot on the surface of the workpiece is irradiated by UVLP as shown in Fig. 1 (b), in which the lens vibrates at the ultrasonic frequency with amplitude A. At the ultrasonic vibration condition, the distance from polished surface to the waist of the output laser z' and the radius of the beam waist $R'_{(z)}$ are respectively:

$$z' = z_l - \frac{F_a \cdot [z_i + A \cdot \sin(2\pi ft)] \cdot [z_i + A \cdot \sin(2\pi ft) - F_a]}{[z_i + A \cdot \sin(2\pi ft) - F_a]^2 + f_F^2} - \frac{F_a \cdot f_F^2}{[z_i + A \cdot \sin(2\pi ft) - F_a]^2 + f_F^2} - z_i + A \cdot \sin(2\pi ft) \tag{15}$$

$$R'_{(z)} = \frac{\sqrt{\left(\pi \cdot R_i^2 \cdot F_a^2\right)^2 + \left\{\lambda \cdot z' \cdot \left[\left(z'_i - F_a\right)^2 + f_F^2\right]\right\}^2}}{\pi \cdot R_i \cdot F_a \cdot \sqrt{\left(z'_i - F_a\right)^2 + f_F^2}} \tag{16}$$

where A is the ultrasonic vibration amplitude, f is ultrasonic frequency, $z_l = z_i + z_0 + z$.

As a result, the energy density of UVLP is expressed as:

$$I_u(z') = \frac{2P \cdot \pi \cdot R_i^2 \cdot F_a^2 \cdot \left[\left(z'_i - F_a\right)^2 + f_F^2\right]}{\left(\pi \cdot R_i^2 \cdot F_a^2\right)^2 + \lambda^2 \cdot z'^2 \cdot \left[\left(z'_i - F_a\right)^2 + f_F^2\right]^2} \tag{17}$$

where $z'_i = z_i + A \times \sin(2\pi ft)$.

Based on the law of conservation of energy, the molten pool on the surface of 304 stainless steel can be kept in equilibrium state by adjusting the laser power, scanning speed, and focus offset. When the laser is irradiated to the surface of the workpiece. After t_m, the molten pool on the surface of the 304 stainless steel workpiece is in equilibrium. Hence the temperature of the surface Eq. (7) is expressed as follows:

$$T(t) = \begin{cases} T_0 + \left(2AI/K\right) \cdot \sqrt{\alpha t/\pi} & 0 \le t \le t_m \\ T_0 + \left(2AI/K\right) \cdot \sqrt{\alpha t_m/\pi} & t_m \le t \end{cases} \tag{18}$$

The parameters of laser polishing 304 stainless steel in Table 1 are substituted into Eq. (18) to obtain the curve of melting pool temperature changing with the time, as shown in Fig. 2. When the equilibrium temperature is 1681 K,

TABLE 1. Process parameters of simulated laser polishing 304 stainless steel.

P (W)	R_i (cm)	F_a (cm)	λ (nm)	z_i (cm)	z (cm)	f (kHz)
450	0.03	1.5	1064	16	0.9	30

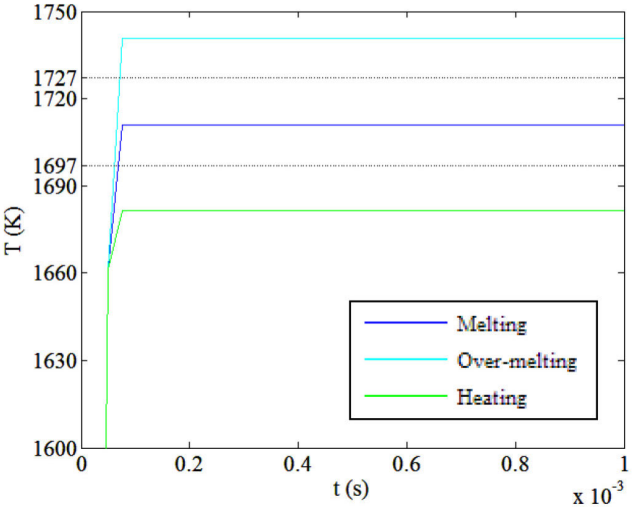

FIGURE 2. The simulation curve of temperature changed with time of 304 stainless steel molten pool polished by TLP.

the curve of molten pool temperature change with time is the green one, as shown in Fig. 2. The temperature is lower than the solidus temperature of the 304 stainless steel material, so the workpiece is in the solid-state with heating marks. The cyan curve shows that the equilibrium temperature of the molten pool is 1741 K higher than the liquidus temperature of the material. At this point, the material of 304 stainless steel is over-melting, and even laser polishing defects such as ablation occur. When the temperature of the molten pool is between the solidus (1697 K) and liquidus (1727 K) lines of the material, it is in a composite state with granular solid uniformly distributed in the liquid phase, as shown the blue curve (1711 K) in Fig. 2.

The ultrasonic vibration lens changed the laser spot diameter on the surface of the 304 stainless steel workpiece and then changed the laser energy density. Substituting Eq. (17) into Eq. (7), the equation of molten pool temperature changed with time by UVLP processing becomes

$$T_u(t) = \begin{cases} T_0 + \left(2AI_u/K\right) \cdot \sqrt{\alpha t/\pi} & 0 \le t \le t_m \\ T_0 + \left(2AI_u/K\right) \cdot \sqrt{\alpha t_m/\pi} & t_m \le t \end{cases} \tag{19}$$

The process and ultrasonic vibration parameters are substituted into Eq. (19) to obtain the curve of the temperature changing with the time of the surface molten pool polished by UVLP, as shown in Fig. 3. Under the action of the ultrasonic vibration lens, the equilibrium temperature in the molten pool is sinusoidal vibration with certain amplitude. Equilibrium temperatures both of the blue and the red curves are 1713 K, which is in the temperature state between the solidus line and liquidus line. When the amplitude is 30 μm, the range of temperature change does not exceed the 304 stainless steel solidus line and liquidus line. Therefore, the molten pool is still in the composite state of solid-liquid coexistence. The amplitude is increased to 60 μm, and the maximum and minimum surface molten pool temperatures

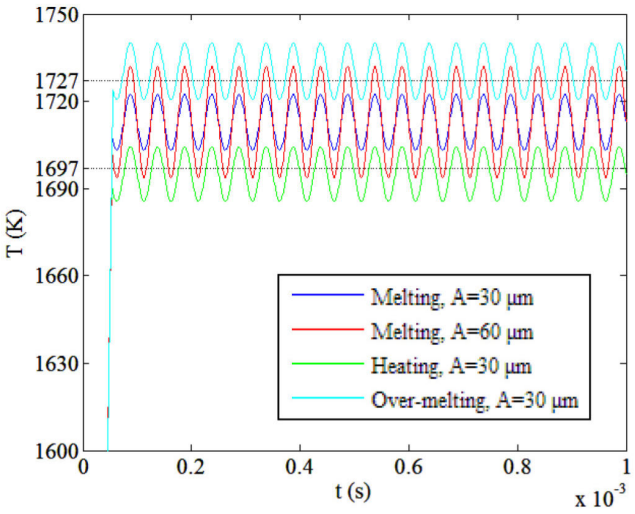

FIGURE 3. The simulation curve of temperature changed with time of 304 stainless steel molten pool polished by UVLP.

are 1732 K and 1694 K, respectively. Under these conditions, it is beyond the temperature range of 1697 K to 1727 K. The laser polishing process of melting-solidification-remelting is formed by repeatedly converted between solid and liquid in the molten pool. The equilibrium temperature of the green curve in Fig. 3 is 1695 K, lower than that of the solidus line. Under the condition of $A = 30$ μm, the temperature range of the molten pool reached 1686 K to 1704 K. Furthermore, the maximum temperature exceeds the solidus temperature. At the same amplitude, the equilibrium temperature of the cyan curve is 1730 K, which makes the molten pool temperature fluctuated between 1721 K and 1739 K.

The theoretical analysis shows that the equilibrium temperature and the range of temperature in the molten pool of 304 stainless steel can be changed by adjusting the laser power, scanning speed, focus offset, and vibration amplitude of UVLP processing. The ultrasonic vibration lens turns the process of the laser polishing metal into the intermittent polishing process, which affects the surface quality of the polished workpiece. Experimental research verifies the result of theoretical analysis and explores the preferred experimental parameters of the UVLP.

III. EXPERIMENTAL CONDITIONS

A. EXPERIMENTAL MATERIALS

Engineered 304 stainless steel has been widely used in medical devices, aerospace, food industry, and other fields due to its excellent corrosion resistance, mechanical properties, high-temperature strength, and high-cost efficiency. In daily use, a humid environment and rough contact surface have a great impact on the useful life of 304 stainless steel. In general, the surface treatment and reduced surface roughness of 304 stainless steel can greatly improve the useful life. The workpiece surface used for experimentation was produced by the wire drawing process and the 3-D surface roughness was 2.777 μm. To facilitate the subsequent microscopic observation and detection, the received 304 stainless steel was cut into 30 mm × 30 mm × 60 mm small blocks by wire EDM. Table 2 presents the performance parameters of the 304 stainless steel.

TABLE 2. The parameters of 304 stainless steel.

Property (unit)	symbol	value
Solidus temperature (K)	T_s	1697
Liquidus temperature (K)	T_l	1727
Density (g·cm^{-3})	ρ	7.2
Melting point (K)	T_m	1700
Boiling point (K)	T_b	3200
Specific heat (J·g^{-1}·K^{-1})	C	0.7118
Initial roughness (μm)	S_a	2.777

B. EXPERIMENTAL EQUIPMENT AND SETUP

The UVLP system is depicted in Fig. 4. It is mainly composed of VMC1100P CNC vertical laser machining center and lens ultrasonic vibration system. 304 stainless steel workpiece is fixed on the moving platform by the clamp. In order to combine the lens ultrasonic vibration device with the VMC1100P CNC vertical laser machining center, a special fixture has been designed. The RIGOL DG811 provides sinusoidal alternating voltage with a frequency of 30 kHz for the lens ultrasonic vibration device. And the Trek PZD350A is used to amplify the input voltage and output it to the ultrasonic vibration transducer. The piezoelectric ceramic converts the electrical signal into the mechanical vibration of ultrasonic frequency, which is amplified by the booster and transmitted to the lens. Finally, UVLP and TLP experiments of 304 stainless steel are completed by this device.

The amplitude of the lens ultrasonic vibration system was measured by the YP0901B amplitude meter, as shown in Fig. 5. Under the condition of not driving the lens ultrasonic vibration device, the measuring head is contacted with the end face of the lens, and the measuring instrument is reset to zero. Then turn on the power to make the lens ultrasonic vibration device generate ultrasonic vibration. At this time, the measured data is the displacement between the peak value and the equilibrium position (i.e., the amplitude value). When the input voltage is constant, different amplitude values can be obtained by adjusting the input frequency. Moreover, the ultrasonic vibration amplitude is the largest at the resonance frequency [35]. The input voltage is set to 150V, and the input frequency range is from 20 kHz to 40 kHz. The amplitude measurement results are shown in Fig. 6. It can be seen from the measurement results that the ultrasonic amplitude of the lens reaches the maximum of 16 μm at 30 kHz. Consequently, 30 kHz is the resonance frequency of the

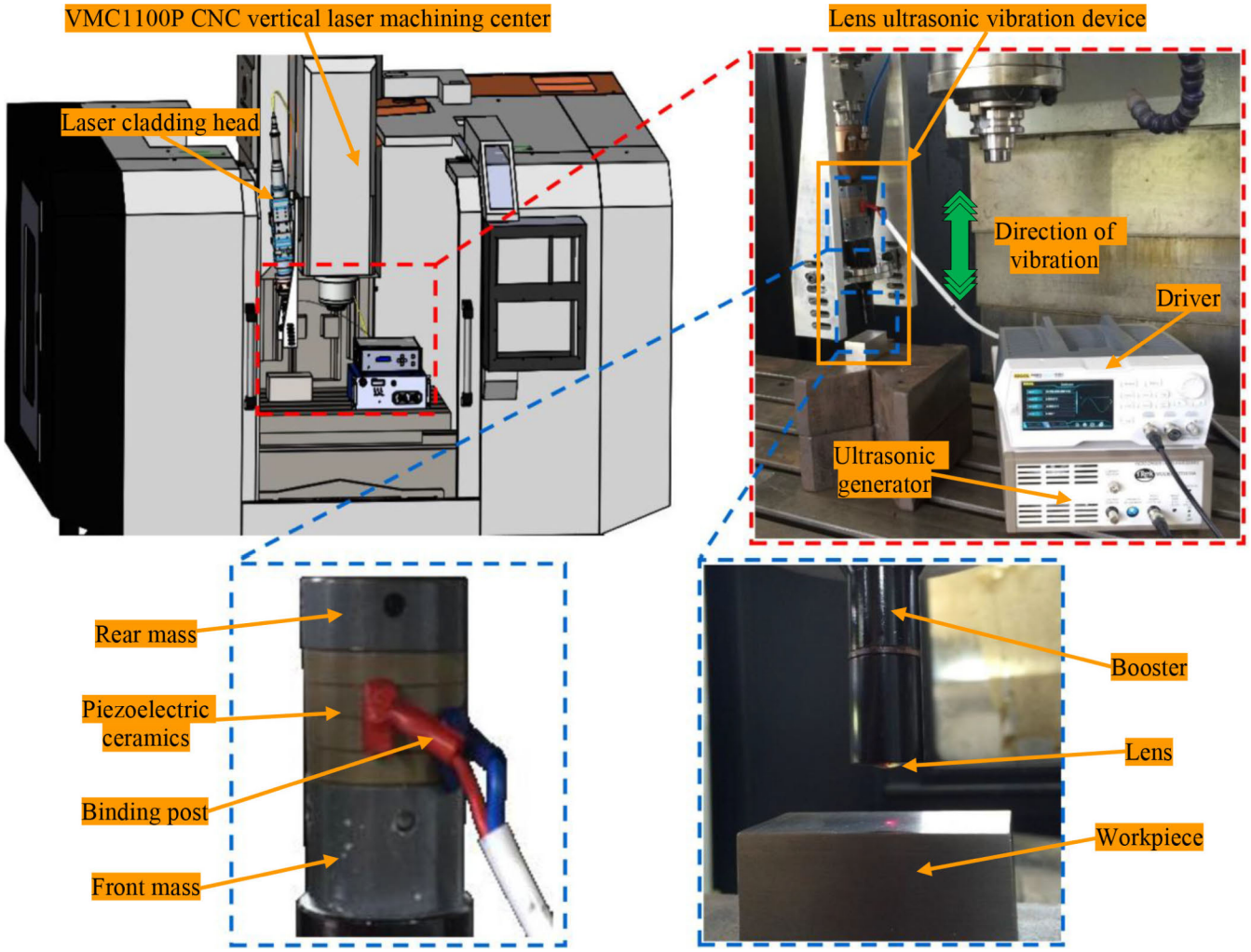

FIGURE 4. Experimental setup for UVLP.

lens ultrasonic vibration device. The amplitude of the lens ultrasonic vibration device is proportional to its input voltage. Under the condition of resonance frequency, the ultrasonic vibration amplitude values corresponding to different input voltages are shown in Table 3.

The scanning speed range of the VMC1100P CNC vertical laser machining center is from 0 to 20000 mm/min. It should be noted that the laser polishing process with a higher scanning speed can prevent excessive accumulation of laser energy on the workpiece surface. The maximum average output power of the laser is 1000 W. Moreover, the laser beam has a Gaussian distribution and the focal diameter is 0.6 mm. The lens ultrasonic vibration device is driven by the ultrasonic generator directly. To achieve the vertical ultrasonic vibration of the lens, and the amplitude range is from 0 to 30 μm. The focal length of the ultrasonic vibration lens is 15 mm. The main conditions of the VMC1100P CNC vertical laser machining center and UVLP system are listed in Table 4.

TABLE 3. Lens ultrasonic vibration device characteristic.

Frequency (kHz)	Voltage (V)	Amplitude (μm)
30	± 45	5
	± 93	10
	± 144	15
	± 202	20
	± 271	25
	± 346	30

IV. EXPERIMENTAL RESULTS

UVLP is an innovative hybrid manufacturing technology at present. The lens vibrates at ultrasonic frequency through the electromechanical conversion characteristics of the piezoelectric ceramic. Therefore, the energy density of the workpiece surface during laser polishing is changed. And the

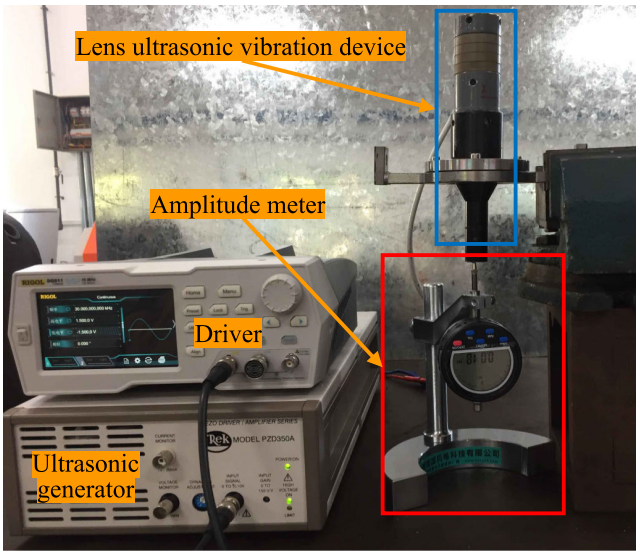

FIGURE 5. Ultrasonic vibration amplitude measurement.

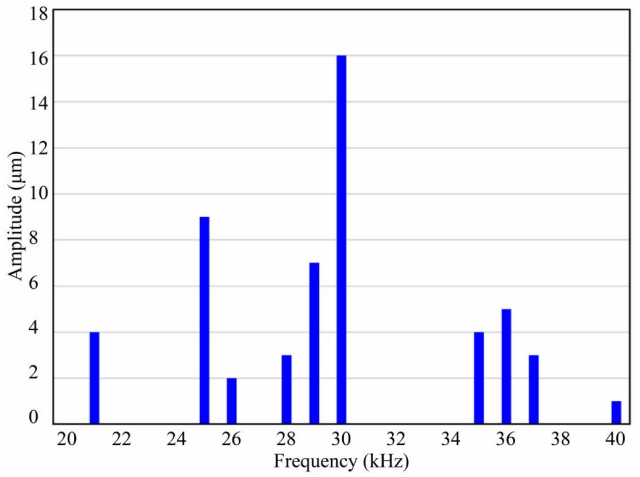

FIGURE 6. Resonance frequency determined by measuring the amplitudes of lens ultrasonic vibration device with different frequencies (at input voltage of 150V).

intermittent laser polishing process is obtained by adjusting the ultrasonic vibration amplitude, laser power, scanning speed, and focus offset. In order to analyze the potential of the UVLP and TLP process, a series of experimental tests are carried out. The principal process parameters of UVLP are laser power, scanning speed, focus offset, and amplitude. The purpose of the comparative experiment between UVLP and TLP is to find a reasonable machining range for each parameter. And the effect of the ultrasonic vibration lens on the thermal mechanism during laser polishing is verified. It provides objective levels combination of each parameter for the orthogonal experiment. Finally, the preferred combination of parameters for ultrasonic vibration-assisted laser polishing 304 stainless steel is obtained by the orthogonal experiment.

TABLE 4. VMC1100P CNC vertical laser machining center and UVLP system conditions.

Parameters	Value
Scanning speed range	0 to 20000 mm·min^{-1}
Operational mode	Continuous-wave laser
Wave length	1064 nm
Maximum power	1000 W
Focus spot diameter	0.6 mm
Voltage range	0 to ± 350 V
Amplitude range	0 to 30 μm
Focal length of lens	15 mm
Output frequency	0 to 10 MHz

A. THE COMPARATIVE EXPERIMENT BETWEEN UVLP AND TLP

The surface roughness and surface morphology are important indexes to measure the surface quality of 304 stainless steel after polishing. In this research, the MiCROMEASUR2 is used to measure the surface roughness (S_a) after polishing. And the KEYENCE VHX-1000E super-depth microscope is used to observe the surface morphology by amplified 100 times and 500 times, respectively. The experimental parameters and the average of the surface roughness obtained from UVLP and TLP are presented in Table 5.

Typical surface morphologies images of the 304 stainless steel polished by UVLP and TLP at $P = 550$ W and $z = 0.7$ cm are shown in Fig. 7. There are some deposits on the surface after polishing at $V = 0.9$ m/min. Combined with the theoretical analysis of the thermal mechanism, the equilibrium temperature of the molten pool is higher than the liquidus temperature of the 304 stainless steel. As shown in Fig. 7 (a) and (b), the ablation and deposit of re-solidified are reduced with the ultrasonic vibration. Fig. 7 (c) presents the surface figure after TLP processing at $V = 2.1$ m/min. It indicates that the equilibrium temperature of the molten pool is lower than the solidus temperature. Some corrugations are observed due to the influence of the Gaussian laser beam with the higher energy density in the center of the polished track. The ablation in the center of the workpiece surface is obviously improved under the condition of ultrasonic vibration, as shown in Fig. 7 (d). The intermittent laser polishing process of UVLP makes the polished 304 stainless steel surface heated more evenly.

Fig. 8 shows the histograms of surface morphology height distribution after UVLP and TLP processing at $P = 550$ W, $z = 0.7$ cm, and different scanning speed. As shown in Fig. 8 (a), when $V = 0.9$ m/min, the surface height distribution range after TLP processing is mainly from -4 μm to 4 μm. Comparing with Fig. 8 (a), the surface height distribution range is reduced to -3 μm to 3 μm under the influence

TABLE 5. 304 stainless steel surface roughness in UVLP and TLP used for experimental results.

No.	Process parameter				Results
	Laser Power P (W)	Scanning Speed V (m/min)	Focus Offset z (cm)	Amplitude A (μm)	Roughness $\bar{S}_a$ (μm)
1	550	0.3	0.7	0	1.540
2	550	0.9	0.7	0	1.064
3	550	1.5	0.7	0	1.381
4	550	2.1	0.7	0	1.653
5	550	2.7	0.7	0	2.104
6	550	0.3	0.7	15	1.258
7	550	0.9	0.7	15	0.874
8	550	1.5	0.7	15	1.569
9	550	2.1	0.7	15	1.822
10	550	2.7	0.7	15	2.319
11	350	1.5	0.7	0	2.603
12	450	1.5	0.7	0	1.906
13	650	1.5	0.7	0	0.823
14	750	1.5	0.7	0	1.155
15	350	1.5	0.7	15	2.747
16	450	1.5	0.7	15	1.995
17	650	1.5	0.7	15	0.720
18	750	1.5	0.7	15	0.982
19	550	1.5	0.5	0	1.126
20	550	1.5	0.6	0	0.855
21	550	1.5	0.8	0	2.008
22	550	1.5	0.9	0	2.352
23	550	1.5	0.5	15	0.989
24	550	1.5	0.6	15	0.755
25	550	1.5	0.8	15	2.177
26	550	1.5	0.9	15	2.633
27	550	1.5	0.7	5	1.423
28	550	1.5	0.7	10	1.499
29	550	1.5	0.7	20	1.645
30	550	1.5	0.7	25	1.689

of ultrasonic vibration, as shown in Fig. 8 (b). Under this machining parameter, the intermittent laser polishing caused by ultrasonic vibration reduces the ablation and evaporation on the surface of the 304 stainless steel, so the average surface morphology height is descended. When the scanning speed is 2.1 m/min, the surface height distribution range after TLP and UVLP processing is -4 μm to 6 μm and -7 μm to 6 μm, respectively, as shown in Fig. 8 (c) and (d). Because the ultrasonic vibration decreases the average laser energy density of the Gaussian laser beam, the melting degree of the workpiece surface is reduced. As a result, the average surface height after the UVLP processing is higher than the TLP.

The 3-D surface morphologies of polished 304 stainless steel surface tested by the MiCROMEASUR2, as shown in Fig. 9. It is noticed that the 3-D surface morphologies in UVLP are different from those in TLP. As can be seen from Fig. 9 (a) and (b), convex and concave parts on the surface are exceedingly irregular after TLP processing. More serious peaks and valleys are formed on the re-solidified surface as a result of the material over-melting and evaporation in TLP. The polished surface has better consistency after the UVLP processing, so the surface roughness can be further declined. As shown in Fig. 9 (c) and (d), there are still many grooves on the surface of the 304 stainless steel after UVLP and TLP processing, which is formed by the traditional cutting tools. It is shown that the lower laser energy density fails to melt the material of the surface sufficiently. The melting degree of the surface morphology polished by UVLP is lower than TLP, as shown in Fig. 9 (d).

Fig. 10 shows the 304 stainless steel surface images after TLP and UVLP processing at $V = 1.5$ m/min, $z = 0.7$ cm, $P = 350$ W, and $P = 650$ W. When the laser power is 350 W, both TLP and UVLP only generate heating traces on the surface of the workpiece, which has little effect on the surface quality improvement, as shown in Fig. 10 (a) and (b). Compared with the lower laser power, the surface quality of the workpiece has been extremely improved by laser polishing at $P = 650$ W. Fig. 10 (c) presents the surface morphology after TLP processing at $P = 650$ W. According to the above theoretical analysis, the equilibrium temperature of the molten pool is between the solidus temperature and liquidus temperature. There are only a few re-solidified micro-particles and cavities in the center of the polished track. The ultrasonic vibration amplitude of 15μm changes the temperature in the molten pool within a certain range. It can be observed from Fig. 10 (d) that there is almost no particle and cavity on the surface after UVLP machining. The surface of the workpiece only has some re-solidified imprints under this polishing condition.

As shown in Fig. 11 (a) and (b), the grooves on the 304 stainless steel almost have no change after UVLP and TLP at $V = 1.5$ m/min, $P = 350$ W, and $z = 0.7$ cm. That means the laser energy density is too small to melt the 304 stainless steel material. The peaks and valleys of the polished surface are significantly reduced by the TLP at $V = 1.5$ m/min, $P = 650$ W, and $z = 0.7$ cm, as shown in Fig. 11 (c). Under the condition of this machining parameter, it is helpful to melt the convex parts on the workpiece surface to fill the concave parts and form a smooth polished surface. The height of peaks and valleys on the workpiece surface are further declined and distributed evenly with the ultrasonic vibration lens, as shown in Fig. 11 (d). The experimental results show

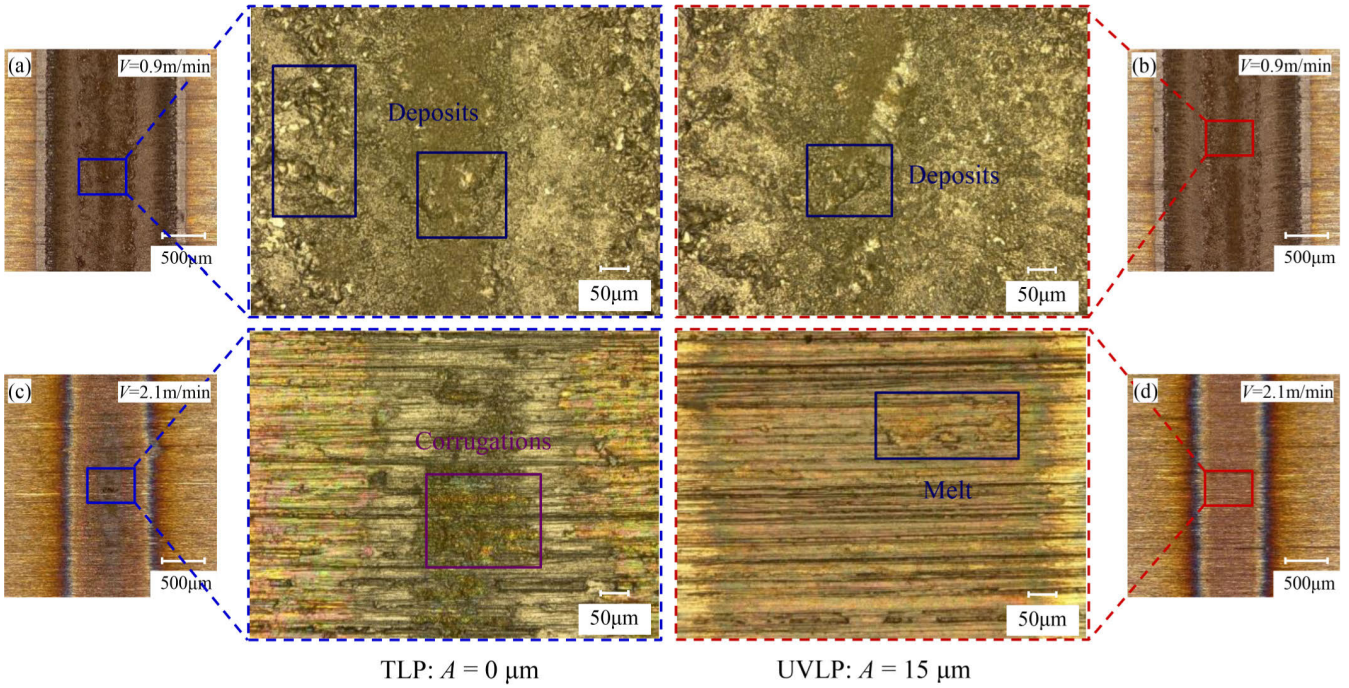

FIGURE 7. Comparison of the surface morphology with different scanning speed at $P = 550$ W and $z = 0.7$ cm. (a) TLP: $V = 0.9$ m/min; (b) UVLP: $V = 0.9$ m/min; (c) TLP: $V = 2.1$ m/min; (d) UVLP: $V = 2.1$ m/min.

that the ultrasonic vibration lens can change the TLP process into the intermittent laser polishing process.

Fig. 12 shows the effect of different focus offset on the laser polishing of the 304 stainless steel. It can be observed from Fig. 12 (a) that there are some re-solidified deposits and particles on the polished surface by TLP at $V = 1.5$ m/min, $z = 0.5$ cm, and $P = 550$ W. Due to the small distance of focus offset, resulting in excessive ablation and other defects of the polished surface. UVLP processing reduces the re-solidified deposits and particles on the surface of the polished workpiece, as shown in Fig. 12 (b). With the increase of focus offset to 0.9 cm, the laser energy density failed to achieve the desired polishing effect, as shown in Fig. 12 (c) and (d). The ultrasonic vibration lens diminishes the average laser energy density, so the melting degree of the workpiece surface is declined by comparing Fig. 12 (c) and Fig. 12 (d).

The mechanism of laser polishing is relocated the melted material of the shallow surface from the peaks to valleys. According to the surface morphology of the polished workpiece, the state of the molten pool in the laser polishing process is judged. The value of surface roughness is a quantitative analysis method to evaluate the surface quality of the workpiece. Therefore, the theoretical analysis results can be verified by combining the surface morphology and surface roughness of the workpiece after laser polishing. As shown in the experimental results, the polished 304 stainless steel surface is heated, melted, or over-melted by adjusting the parameters of laser power, scanning speed, and focus offset. When the laser power is 650 W, the scanning speed is 1.5 m/min, and the focus offset is 0.7cm, the polished 304 stainless steel surface is melting, as shown in Fig. 10 (c). The intermittent UVLP processing is formed after the ultrasonic vibration lens is applied with the 15 μm amplitude. Furthermore, the melting state in the molten pool is changed and the surface quality of polished 304 stainless steel is improved, as shown in Fig. 10 (d). As a result, the theoretical model is verified by the comparative experiment between TLP and UVLP.

B. ORTHOGONAL EXPERIMENT

The orthogonal experimental design is an important method to deal with multi-factor experimental research, which is scientific, simple, and effective. At the same time, the experimental factors are arranged effectively and reasonably to minimize experimental errors. So as to realize the purpose of rapid, efficient, and economical experiment. The experiment in this article includes four factors, and four levels are selected for each factor. The preferred parameters can be obtained by the full permutation test. However, due to the limitation of the test period and cost, the full permutation test cannot be selected. Therefore, in this research, the orthogonal experiment is conducted to study the ultrasonic vibration-assisted laser polishing of 304 stainless steel. The aim is to obtain the preferred combination of process parameters and make the surface quality better. According to the result of the comparative experiment, four levels of each factor are selected, as shown in Table 6.

Based on the combination of factors and levels determined in Table 6, the level number of factors is consistent with the level number of the orthogonal table. The principle of

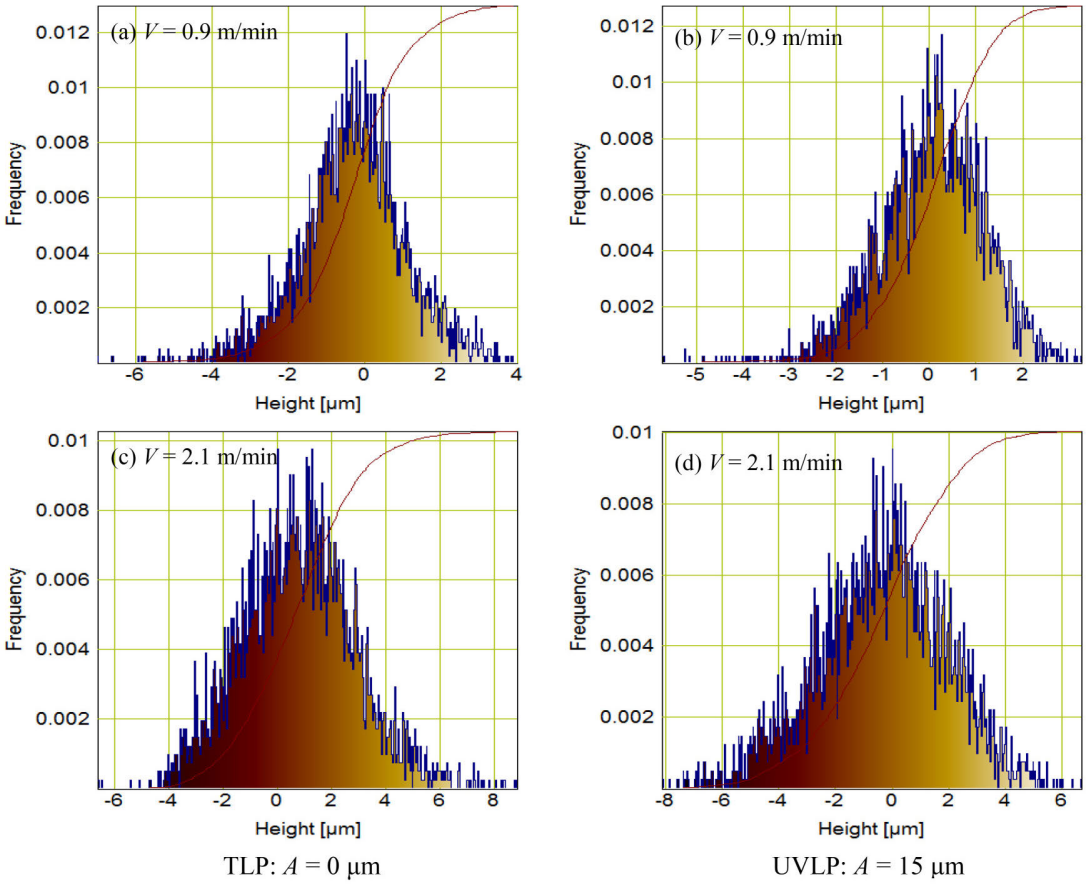

FIGURE 8. Height distribution histograms at $P = 550$ W and $z = 0.7$ cm. (a) TLP: $V = 0.9$ m/min; (b) UVLP: $V = 0.9$ m/min; (c) TLP: $V = 2.1$ m/min; (d) UVLP: $V = 2.1$ m/min.

TABLE 6. Factors and levels of orthogonal experiment.

Factors	Laser Power P (W)	Scanning Speed V (m/min)		Focus Offset z (cm)	Amplitude A (μm)
Levels	1	400	0.3	0.6	10
	2	500	0.9	0.7	15
	3	600	1.5	0.8	20
	4	700	2.1	0.9	25

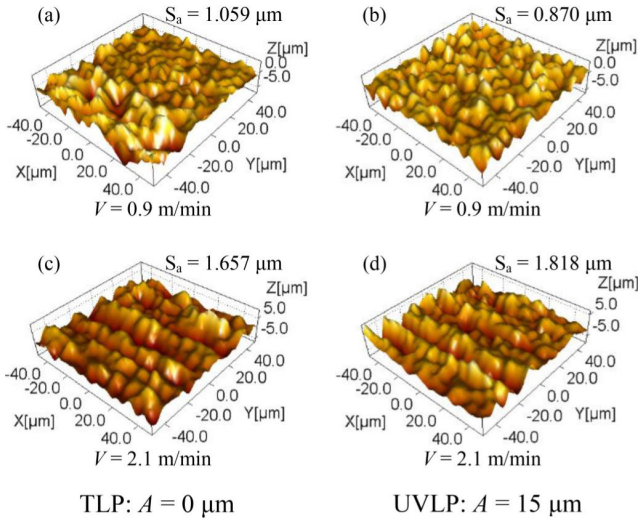

FIGURE 9. 3-D surface morphologies at $P = 550$ W and $z = 0.7$ cm. (a) TLP: $V = 0.9$ m/min; (b) UVLP: $V = 0.9$ m/min; (c) TLP: $V = 2.1$ m/min; (d) UVLP: $V = 2.1$ m/min.

choosing the orthogonal table is as follows. Under the premise that the experimental factors can be arranged, a small orthogonal table is chosen as far as possible to reduce the number of tests. In addition, in order to investigate the experimental error, it is best to have an empty column after arranged the experimental factors in the selected orthogonal table. Otherwise, the repeated experiment must be carried out to study the experimental error. L_n (m^k) is the format of the orthogonal table, where L is the symbol of the orthogonal table, n is the number of lines in the orthogonal table, k is the number of columns in the orthogonal table, and m is the level number of each factor. In this article, the orthogonal table L_{16} (4^5) is selected without interaction and the result of the orthogonal experiment is shown in Table 7.

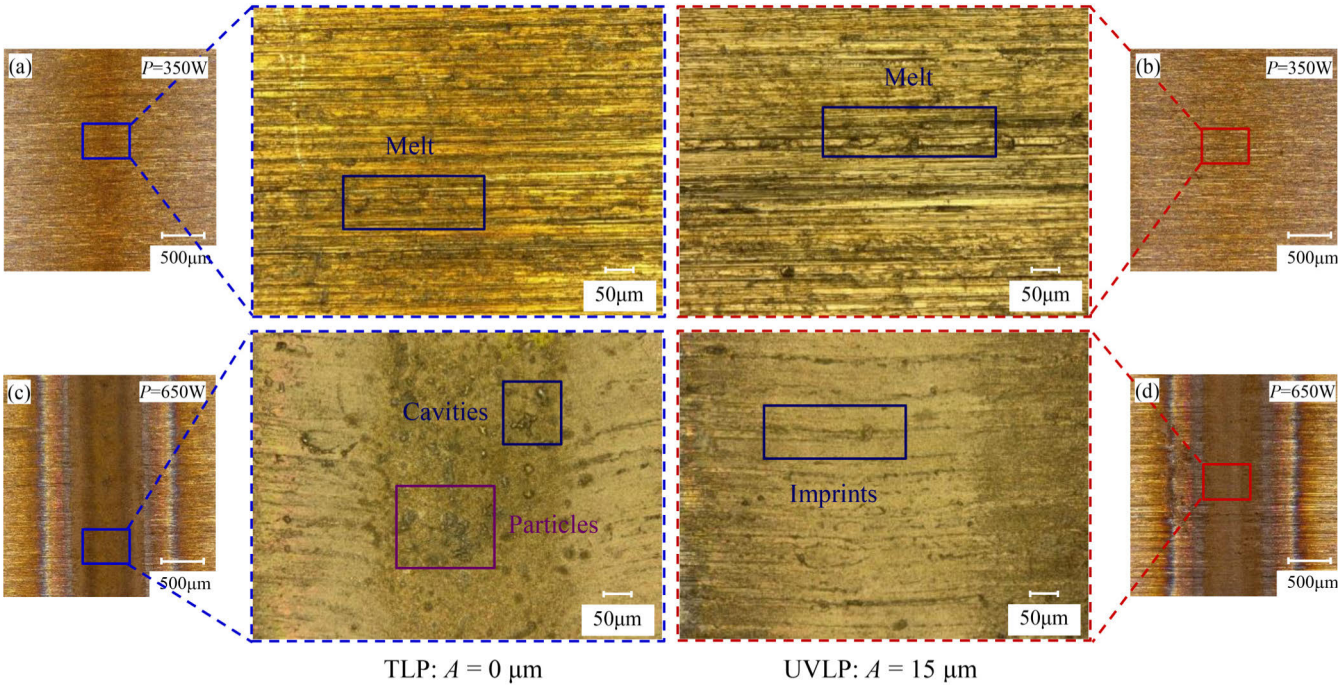

FIGURE 10. Comparison of the surface morphology with different laser power at $V = 1.5$ m/min and $z = 0.7$ cm. (a) TLP: $P = 350$ W; (b) UVLP: $P = 350$ W; (c) TLP: $P = 650$ W; (d) UVLP: $P = 650$ W.

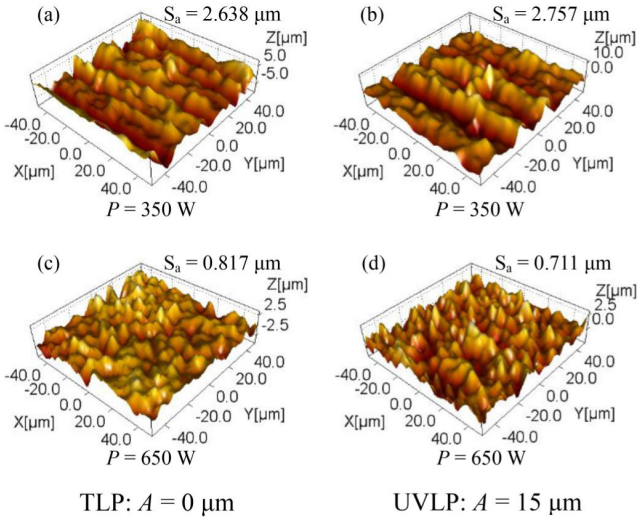

FIGURE 11. 3-D surface morphologies at $V = 1.5$ m/min and $z = 0.7$ cm. (a) TLP: $P = 350$ W; (b) UVLP: $P = 350$ W; (c) TLP: $P = 650$ W; (d) UVLP: $P = 650$ W.

TABLE 7. Results of the orthogonal experiment.

No.	P (W)	V (m/min)	z (cm)	A (μm)	Error column	S_a (μm)
1	400	0.3	0.6	10	1	1.042
2	400	0.9	0.7	15	2	2.207
3	400	1.5	0.8	20	3	2.695
4	400	2.1	0.9	25	4	2.773
5	500	0.3	0.7	20	4	1.354
6	500	0.9	0.6	25	3	0.977
7	500	1.5	0.9	10	2	2.380
8	500	2.1	0.8	15	1	2.386
9	600	0.3	0.8	25	2	1.080
10	600	0.9	0.9	20	1	1.387
11	600	1.5	0.6	15	4	0.865
12	600	2.1	0.7	10	3	1.598
13	700	0.3	0.9	15	3	2.401
14	700	0.9	0.8	10	4	0.919
15	700	1.5	0.6	25	1	0.736
16	700	2.1	0.7	20	2	0.711

V. DISCUSSION

A. INFLUENCE OF THE EXPERIMENTAL PARAMETERS ON THE 304 STAINLESS STEEL POLISHED BY UVLP AND TLP

Fig. 13 illustrates the influence of scanning speed on the polished surface roughness in TLP and UVLP processing. As the scanning speed increases from 0.3 m/min to 2.7 m/min, the surface roughness after TLP and UVLP processing decreases first and then increases when $P = 550$ W and $z = 0.7$ cm. After TLP and UVLP processing, the surface roughness reaches the minimum value of 1.064 μm and 0.874 μm respectively when the scanning speed is 0.9 m/min.

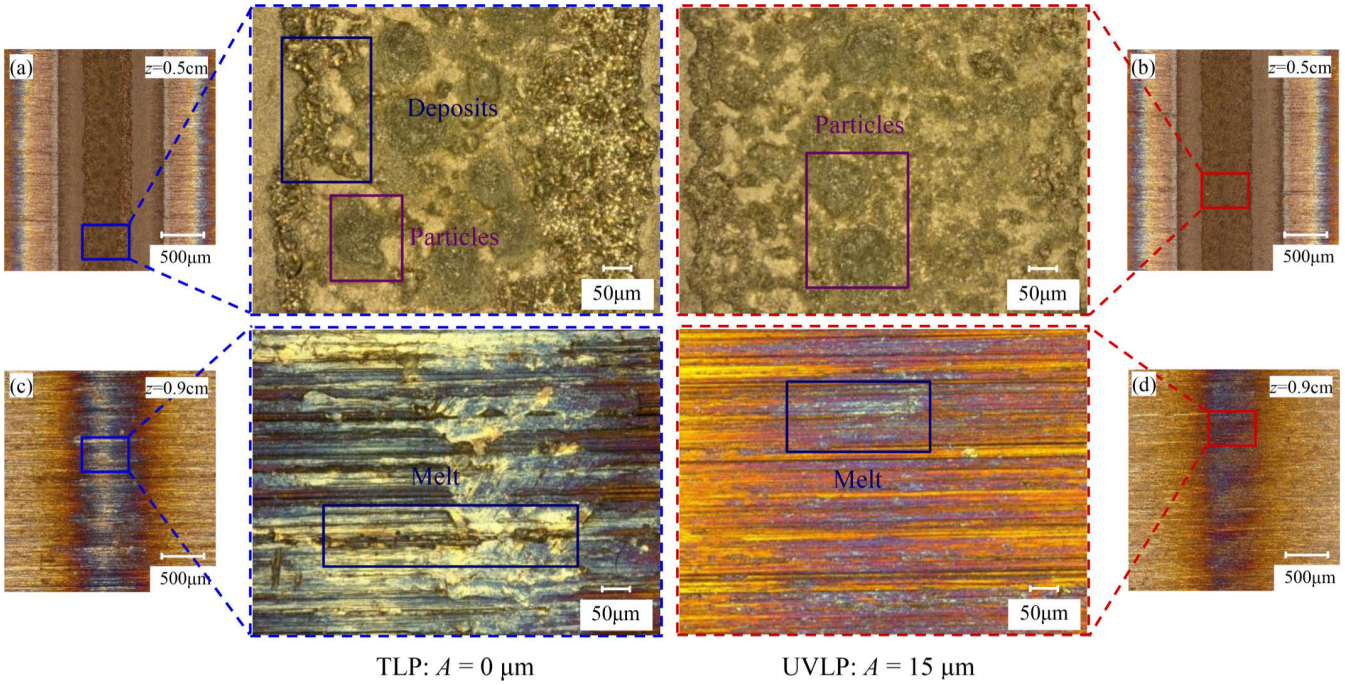

FIGURE 12. Comparison of the surface morphology with different focus offset at $V = 1.5$ m/min and $P = 550$ W (a) TLP: $z = 0.5$ cm; (b) UVLP: $z = 0.5$ cm; (c) TLP: $z = 0.9$ cm; (d) UVLP: $z = 0.9$ cm.

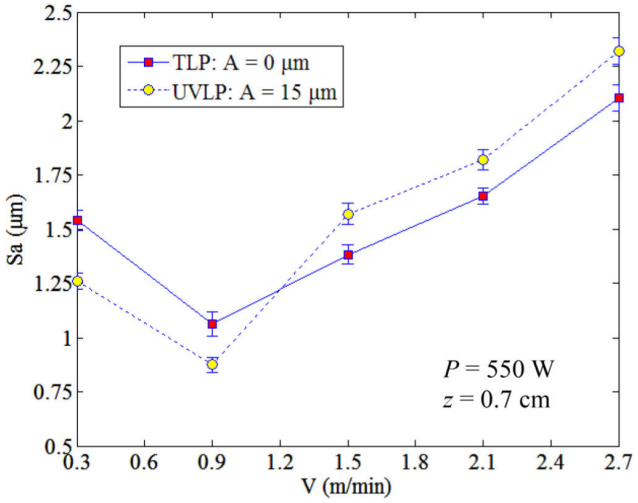

FIGURE 13. Effect of scanning speed on the polished surface roughness in TLP and UVLP processing. The error bars are standard deviation based on three repetitions measured data.

When the scanning speed is less than 0.9 m/min, the workpiece surface is ablated. Ultrasonic vibration reduces the ablation and makes the roughness of UVLP lower than that of TLP. As the scanning speed is higher than 1.5 m/min, the laser energy density is insufficient to melt the surface of 304 stainless steel completely. Consequently, the roughness is higher than TLP due to the influence of intermittent polishing that is caused by ultrasonic vibration.

The relationship between laser power and surface roughness after TLP and UVLP processing at the same scanning speed and focus offset is shown in Fig. 14. When $V = 1.5$ m/min, $z = 0.7$ cm, and the laser power raised from 350 W to 750 W, the melting degree of the polished 304 stainless steel surface gradually is increased after TLP and UVLP processing. The surface roughness of 304 stainless steel is polished by TLP and UVLP to reach the valley value of 0.720 μm and 0.823 μm at $P = 650$ W, respectively. As the laser power is less than 550 W, the Gaussian laser beam does not form a molten pool on the workpiece surface.

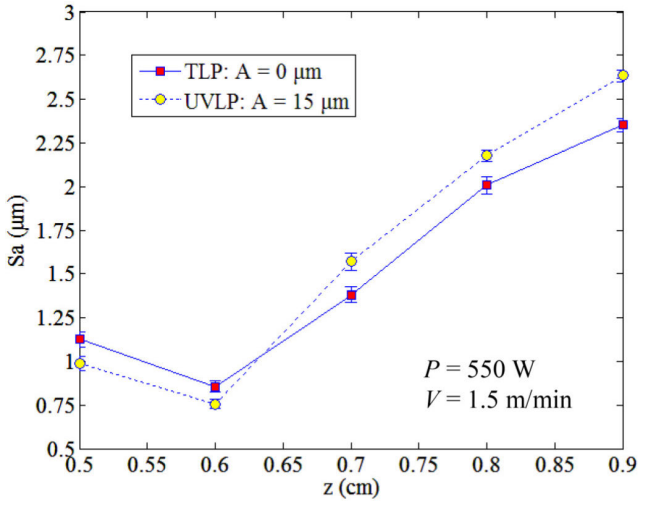

FIGURE 14. Effect of laser power on the polished surface roughness in TLP and UVLP processing. The error bars are standard deviation based on three repetitions measured data.

As a result, the surface roughness after TLP processing is lower than that of UVLP processing. The ablation and excessive evaporation are formed on the surface of 304 stainless steel when the laser power is higher than 750 W and ultrasonic vibration helps to reduce this phenomenon.

Fig. 15 demonstrates the relationship between focus offset and surface roughness that is polished by TLP and UVLP. In the process of laser polishing, the longer distance of the focus offset, the smaller energy density of Gaussian laser beam on the workpiece surface. Surface roughness of the workpiece after UVLP polished is lower than that of TLP at $P = 550$W, $V = 1.5$ m/min, and focus offset less than 0.6 cm. When the focus offset is greater than 0.7 cm, the ultrasonic vibration reduces the average laser energy density, and the surface roughness after polishing is greater than that of TLP.

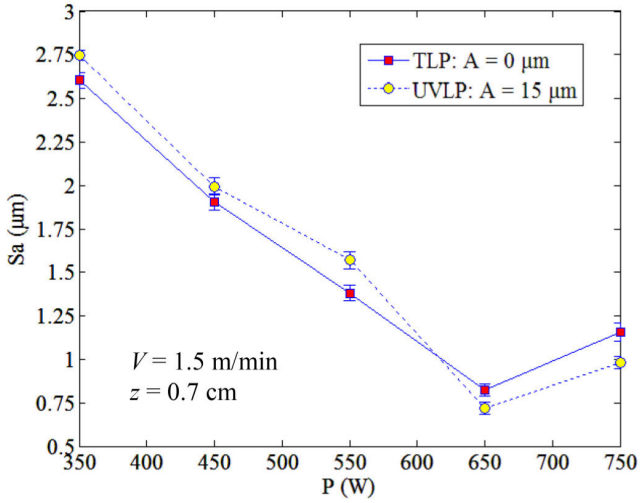

FIGURE 15. Effect of focus offset on the polished surface roughness in TLP and UVLP processing. The error bars are standard deviation based on three repetitions measured data.

B. RANGE ANALYSIS OF ORTHOGONAL EXPERIMENT

Since the orthogonal experiment is a partial test, the preferred experimental parameter combination cannot be guaranteed in the partial test. On the other hand, we also hope to use the information provided by the partial test data to understand the importance and regularity of each factor's influence on the test index. Thus the experimental results must be calculated and analyzed. The range analysis method has the characteristics of simple calculation and intuitionistic. And the following conclusions can be obtained from the analysis of orthogonal experimental results by range analysis method: 1) factors influence order affecting or main factors, 2) preferred combination of experimental levels for desired quality characteristics [36]. There are two important index parameters in the range analysis, which are K_{ij} and R_i respectively. The summation of the experimental index of level j for the factor i is K_{ij}. The mean value of K_{ij} is K_{ij}/k_j and it is the parameter for determining the preferred combination, where k_j is the number of levels on any column. R_i is the range, which is the difference between the maximum and minimum values of levels in a list of factors. R_i is used to evaluate the importance of each factor [37].

The general form of calculating equation for K_{ij}, K_{ij}/k_j, and R_i are described as [38]:

$$K_{ij}/k_j = \frac{1}{k_j} \cdot \sum_{i=1}^{k_j} x_{ij} \tag{20}$$

$$R_i = \max(K_{i1}, K_{i2}, \ldots, K_{im}) - \min(K_{i1}, K_{i2}, \ldots, K_{im}) \tag{21}$$

where i is the notation of factors (I, II, III, IV, or V in this research), j is the notation of levels (1, 2, 3, or 4 in this study), x_{ij} is the experimental value for factor i in level j.

By substituting the orthogonal experimental results into Eq. (20) and Eq. (21), the range analysis results of the surface roughness of the 304 stainless steel after UVLP processing are shown in Table 8 and Fig. 16. In this article, the index value is surface roughness S_a, and the minimum value of each factor corresponds to the optimal level, which is K_{I3}, K_{II3}, K_{III2}, K_{IV3}, respectively. R_i reflects the influence of the factor on the experimental indicators. Therefore, according to the range R_i, the influence of UVLP processing factors on the surface roughness of the 304 stainless steel is ranked as follows: Laser Power > Focus Offset > Amplitude > Scanning Speed.

TABLE 8. Surface roughness range analysis.

	i / j	Laser Power I	Scanning Speed II	Focus Offset III	Amplitude IV	Error column V
K_{ij}	1	9.483	6.883	5.277	6.682	6.654
	2	7.374	6.660	5.268	7.859	6.101
	3	4.328	6.256	7.456	5.907	7.383
	4	5.480	6.866	8.664	6.217	6.527
k_j		4	4	4	4	4
K_{i1}/k_j		2.371	1.721	1.319	1.671	1.664
K_{i2}/k_j		1.844	1.665	1.317	1.965	1.525
K_{i3}/k_j		1.082	1.564	1.864	1.477	1.846
K_{i4}/k_j		1.370	1.717	2.166	1.554	1.632
Optimum level		K_{I3}	K_{II3}	K_{III2}	K_{IV3}	K_{V2}
R_i		5.155	0.627	3.509	1.952	1.282

C. VARIANCE ANALYSIS OF ORTHOGONAL EXPERIMENT

According to the range analysis above, the influence of four experimental factors on the test index of ultrasonic vibration-assisted laser polishing 304 stainless steel was determined. However, it is necessary to identify whether the influence of experimental factors on the test index is significant and real with the variance analysis [39]. The principle of variance

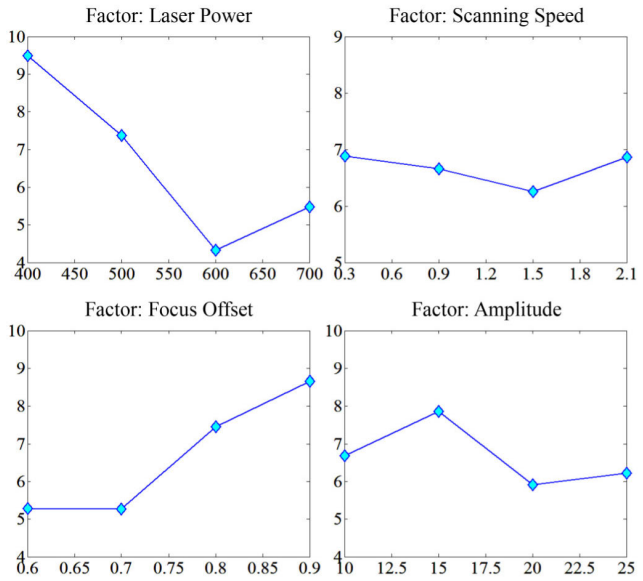

FIGURE 16. Relationship between factors and experimental indicators.

analysis is the difference in the mean of different experiment groups that is caused by experimental conditions and errors. The ratio of the mean-squared deviation of each factor to that of the experimental error is expressed by the F-value. It is used to express the significance of each factor and the data analysis.

The sum of square deviation for each factor (written as SS_i), the total sum of square deviation (written as SS_T), and the sum of square deviation for experimental error (written as SS_E) which can be calculated as follows:

$$SS_i = \frac{m}{n} \cdot \sum_{j=1}^{m} K_{ij}^2 - \frac{1}{n} \cdot \left(\sum_{i=1}^{k} \sum_{j=1}^{m} x_{ij} \right)^2 \tag{22}$$

$$SS_T = \sum_{i=1}^{k} \sum_{j=1}^{m} x_{ij}^2 - \frac{1}{n} \cdot \left(\sum_{i=1}^{k} \sum_{j=1}^{m} x_{ij} \right)^2 \tag{23}$$

$$SS_E = SS_T - \sum_{i=1}^{k} SS_i \tag{24}$$

From Eq. (22) and Eq. (24), the mean-square deviation of each factor (MS_i) and the mean-square deviation experimental error (MS_E) can be obtained as:

$$MS_i = \frac{SS_i}{DF_i} \tag{25}$$

$$MS_E = \frac{SS_E}{DF_E} \tag{26}$$

where DF_i is the degree of freedom for each factor and DF_E is the degree of freedom for experimental error.

The F-value of each factor (F_i) is expressed as:

$$F_i = \frac{MS_i}{MS_E} \tag{27}$$

The above equations are used to calculate the orthogonal experiment results in Table 7. And the variance analysis results of the surface roughness after UVLP processing are listed in Table 9. According to this table, the significance of each factor on the surface roughness of 304 stainless steel after UVLP processing can be determined specifically. The F-value of the laser power and the focus offset are 27.635 and 15.392 respectively, as shown in Table 9. They are higher than the F-critical value of $F_{0.01}$. Thus the influence of laser power and focus offset on the experiment results is regarded as highly significant. Similarly, the F-value of the factor amplitude is 3.973. It is higher than the F-critical value of $F_{0.1}$, so the effect of amplitude on the surface roughness polished by UVLP is treated as significant. However, the impact of the scanning speed on the 304 stainless steel surface roughness (S_a) is insignificant, as shown in Table 9. The results of variance analysis are consistent with the results of range analysis, therefore, the preferred combination of process parameters for ultrasonic vibration-assisted laser polishing 304 stainless steel is: Laser Power $=$ 600 W; Scanning Speed $=$ 1.5 m/min; Focus Offset $=$ 0.7 cm; Amplitude $=$ 20 μm.

TABLE 9. Surface roughness variance analysis.

Factor	Laser Power	Scanning Speed	Focus Offset	Amplitude	Error
SS	3.827	0.064	2.132	0.550	0.277
DF	3	3	3	3	6
MS	1.276	0.021	0.711	0.183	0.046
F	27.635	0.461	15.392	3.973	
$F_{0.01}$	9.78	9.78	9.78	9.78	
$F_{0.05}$	4.76	4.76	4.76	4.76	
$F_{0.1}$	3.29	3.29	3.29	3.29	
Significance	**		**	*	

In order to verify the range analysis and variance analysis results of the orthogonal experiment, the ultrasonic vibration-assisted laser polishing 304 stainless steel experiment under the preferred process parameters is carried out. The KEYENCE VHX-1000E super-depth microscope is used to observe the surface morphology of polished 304 stainless steel by amplified 100 and 500 times respectively, as shown in Fig. 17. The intermittent polishing process of UVLP makes the polished surface more uniform. After the UVLP processing, the surface has no re-solidified cavities and particles. The surface of the 304 stainless steel is more uniform and the surface quality is further improved at $V = 1.5$ m/min, $P = 600$ W, $z = 0.7$ cm, and $A = 20$ μm. Moreover, the 3-D roughness (S_a) of the polished surface is 0.512 μm, 0.527 μm, 0.546 μm, and 0.530 μm respectively, which is measured by the MiCROMEASUR2. Compared with the initial surface roughness of $S_a = 2.777\mu$m, the surface

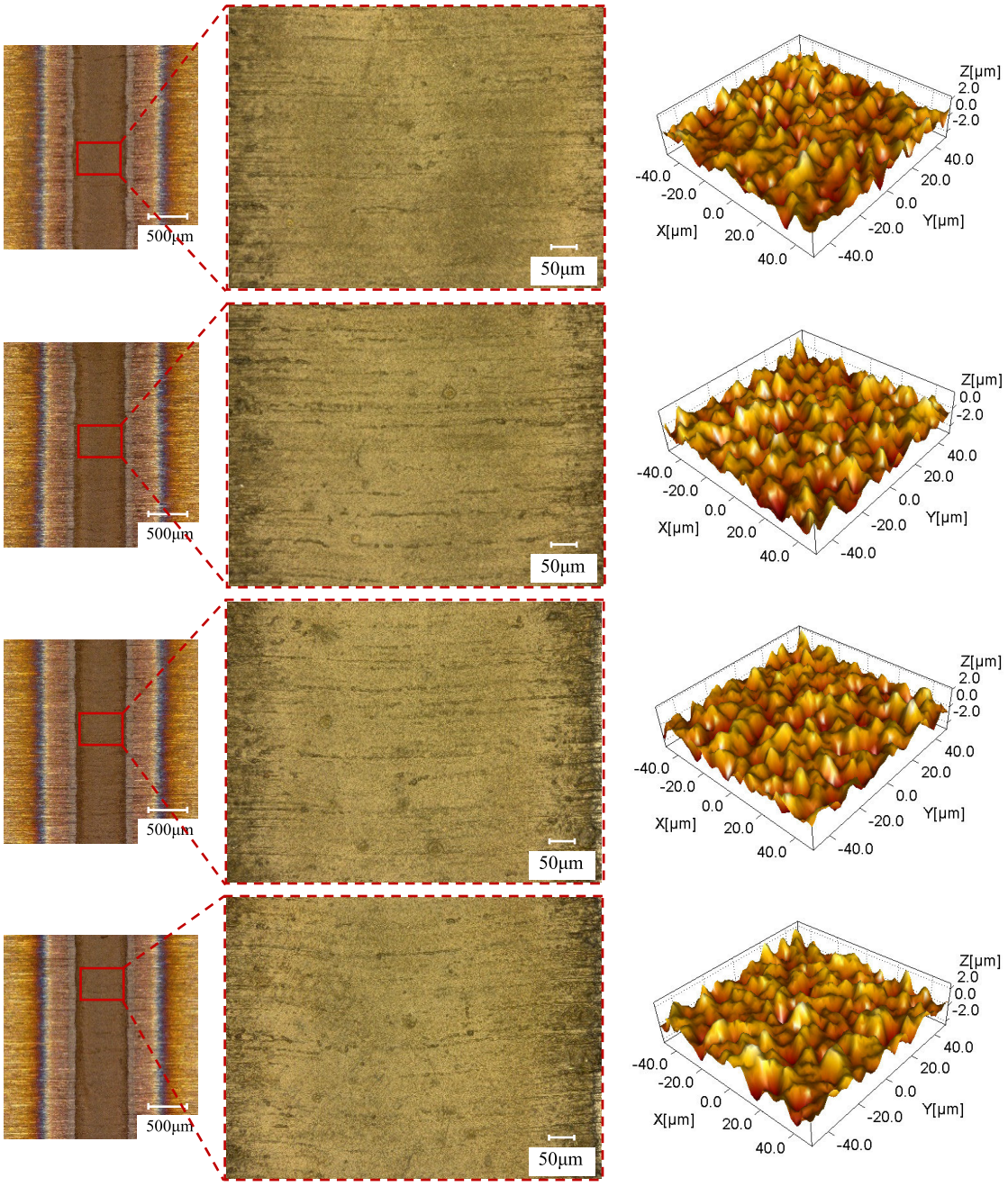

FIGURE 17. Surface morphologies of the polished 304 stainless steel at $V = 1.5$ m/min; $P = 600$ W; $z = 0.7$ cm; $A = 20$ μm.

roughness of 304 stainless steel after UVLP processing can be reduced by 81% under the preferred parameters. Therefore, the ultrasonic vibration lens can improve the surface quality of laser polishing 304 stainless steel.

VI. CONCLUSION

This study presents the UVLP method to polish 304 stainless steel. The energy distribution in the spot on the workpiece surface is changed by controlling the ultrasonic vibration lens. In this way, the surface quality of the workpiece after UVLP processing is further improved. Moreover, the method is verified by theoretical analysis and experimental work. The major conclusions are summarized as follows:

(1) A method of laser polishing by piezoelectric ceramic driven lens was presented, and an experimental platform of UVLP polishing 304 stainless steel was built. The thermal mechanism analysis has shown that both equilibrium temperature and the range of temperature in the molten pool were changed by adjusting the processing parameters of UVLP, so it affected the roughness of the polished surface.

(2) Comparative experiments between TLP and UVLP have verified the correctness of the theoretical analysis of the thermal mechanism. The ultrasonic vibration lens has changed the surface roughness of 304 stainless steel that was polished by laser. And the level range of each factor was provided for the orthogonal experiment by comparative experiments.

(3) The range analysis and variance analysis of the orthogonal experiment results have shown that the significant order of each experimental factor was: Laser Power > Focus Offset > Amplitude > Scanning Speed. It was found that the preferred combination of process parameters for ultrasonic vibration-assisted laser polishing 304 stainless steel under presented experimental setup was: Laser Power = 600 W; Scanning Speed = 1.5 m/min; Focus Offset = 0.7 cm; Amplitude = 20 μm. Under these optimization parameters, the surface roughness of 304 stainless steel after UVLP treatment was reduced by 81%.

REFERENCES

[1] G. Wang, Z. Liu, J. Niu, W. Huang, and B. Wang, "Effect of electrochemical polishing on surface quality of nickel-titanium shape memory alloy after milling," *J. Mater. Res. Technol.*, vol. 9, no. 1, pp. 253–262, Jan. 2020, doi: 10.1016/j.jmrt.2019.10.053.

[2] Z. Qu, W. Wang, S. Yang, Q. Sun, Z. Fang, and Y. Zheng, "Noncontact thickness measurement of cu film on silicon wafer using magnetic resonance coupling for stress free polishing application," *IEEE Access*, vol. 7, pp. 75330–75341, Jun. 2019, doi: 10.1109/ACCESS.2019.2921005.

[3] T. Zeng and T. Sun, "Size effect of nanoparticles in chemical mechanical polishing—A transient model," *IEEE Trans. Semicond. Manuf.*, vol. 18, no. 4, pp. 655–663, Nov. 2005, doi: 10.1109/TSM.2005.858508.

[4] J. Lin, H. Lu, Y. Gu, X. Zhou, C. Xin, M. Kang, and X. Cang, "A new vibration device applied for two-dimensional ultrasonic polishing of biomaterials," *IEEE Access*, vol. 7, pp. 92838–92849, Jul. 2019, doi: 10.1109/ACCESS.2019.2927615.

[5] C. Ma, M. Vadali, N. Duffie, F. Pfefferkorn, and X. Li, "Melt pool flow and surface evolution during pulsed laser micro polishing of Ti6Al4V," *ASME. J. Manuf. Sci. Eng.*, vol. 135, pp. 061023-1–061023-8, Nov. 2013, doi: 10.1115/1.4025819.

[6] Y. Li, Z. Zhang, and Y. Guan, "Thermodynamics analysis and rapid solidification of laser polished inconel 718 by selective laser melting," *Appl. Surf. Sci.*, vol. 511, May 2020, Art. no. 145423, doi: 10.1016/j.apsusc.2020.145423.

[7] W.-J. Liu, S.-Q. Chen, X.-L. Hu, Z. Liu, J.-Y. Zhang, L.-Y. Ying, X.-Q. Lv, H. Akiyama, Z.-P. Cai, and B.-P. Zhang, "Low threshold lasing of GaN-based VCSELs with sub-nanometer roughness polishing," *IEEE Photon. Technol. Lett.*, vol. 25, no. 20, pp. 2014–2017, Oct. 2013, doi: 10.1109/LPT.2013.2280965.

[8] L. Giorleo, E. Ceretti, and C. Giardini, "Ti surface laser polishing: Effect of laser path and assist gas," *Procedia CIRP*, vol. 33, pp. 446–451, 2015, doi: 10.1016/j.procir.2015.06.102.

[9] A. Temmler, D. Liu, J. Preußner, S. Oeser, J. Luo, R. Poprawe, and J. H. Schleifenbaum, "Influence of laser polishing on surface roughness and microstructural properties of the remelted surface boundary layer of tool steel H11," *Mater. Design*, vol. 192, Jul. 2020, Art. no. 108689, doi: 10.1016/j.matdes.2020.108689.

[10] C. Weingarten, A. Schmickler, E. Willenborg, K. Wissenbach, and R. Poprawe, "Laser polishing and laser shape correction of optical glass," *J. Laser Appl.*, vol. 29, no. 1, Feb. 2017, Art. no. 011702, doi: 10.2351/1.4974905.

[11] F. E. Pfefferkorn, N. A. Duffie, J. D. Morrow, and Q. Wang, "Effect of beam diameter on pulsed laser polishing of s7 tool steel," *CIRP Ann.*, vol. 63, no. 1, pp. 237–240, 2014, doi: 10.1016/j.cirp.2014.03.055.

[12] E. V. Bordatchev, A. M. K. Hafiz, and O. R. Tutunea-Fatan, "Performance of laser polishing in finishing of metallic surfaces," *Int. J. Adv. Manuf. Technol.*, vol. 73, nos. 1–4, pp. 35–52, Apr. 2014, doi: 10.1007/s00170-014-5761-3.

[13] P.-R. Jang, C.-G. Kim, G.-P. Han, M.-C. Ko, U.-C. Kim, and H.-S. Kim, "Influence of laser spot scanning speed on micro-polishing of metallic surface using UV nanosecond pulse laser," *Int. J. Adv. Manuf. Technol.*, vol. 103, nos. 1–4, pp. 423–431, Mar. 2019, doi: 10.1007/s00170-019-03559-8.

[14] E. Ukar, A. Lamikiz, L. N. L. De Lacalle, S. Martinez, F. Liébana, and Tabernero, "Thermal model with phase change for process parameter determination in laser surface processing," *Phys. Procedia*, vol. 5, pp. 395–403, 2010, doi: 10.1016/j.phpro.2010.08.066.

[15] J. Ning, D. E. Sievers, H. Garmestani, and S. Y. Liang, "Analytical modeling of in-process temperature in powder feed metal additive manufacturing considering heat transfer boundary condition," *Int. J. Precis. Eng. Man-Gt*, vol. 7, pp. 1–9, May 2020, doi: 10.1007/s40684-019-00164-8.

[16] E. Kundakcğlu, I. Lazoglu, Ö. Poyraz, E. Yasa, and N. Cizicioğlu, "Thermal and molten pool model in selective laser melting process of inconel 625," *Int. J. Adv. Manuf. Technol.*, vol. 95, nos. 9–12, pp. 3977–3984, Jan. 2018, doi: 10.1007/s00170-017-1489-1.

[17] S. Mohajerani, E. V. Bordatchev, and O. R. Tutunea-Fatan, "Recent developments in modeling of laser polishing of metallic materials," *Lasers Manuf. Mater. Process.*, vol. 5, no. 4, pp. 395–429, Sep. 2018, doi: 10.1007/s40516-018-0071-5.

[18] A. Krishnan and F. Fang, "Review on mechanism and process of surface polishing using lasers," *Frontiers Mech. Eng.*, vol. 14, no. 3, pp. 299–319, Mar. 2019, doi: 10.1007/s11465-019-0535-0.

[19] J. A. Ramos-Grez and D. L. Bourell, "Reducing surface roughness of metallic freeform-fabricated parts using non-tactile finishing methods," *Int. J. Mater. Production Technol.*, vol. 21, no. 4, pp. 297–316, Jan. 2004, doi: 10.1504/IJMPT.2004.004944.

[20] K. C. Yung, S. S. Zhang, L. Duan, H. S. Choy, and Z. X. Cai, "Laser polishing of additive manufactured tool steel components using pulsed or continuous-wave lasers," *Int. J. Adv. Manuf. Technol.*, vol. 105, nos. 1–4, pp. 425–440, Nov. 2019, doi: 10.1007/s00170-019-04205-z.

[21] T. A. Mai and G. C. Lim, "Micromelting and its effects on surface topography and properties in laser polishing of stainless steel," *J. Laser Appl.*, vol. 16, no. 4, pp. 221–228, Nov. 2004, doi: 10.2351/1.1809637.

[22] D. Bhaduri, P. Penchev, A. Batal, S. Dimov, S. L. Soo, S. Sten, U. Harrysson, Z. Zhang, and H. Dong, "Laser polishing of 3D printed mesoscale components," *Appl. Surf. Sci.*, vol. 405, pp. 29–46, May 2017, doi: 10.1016/j.apsusc.2017.01.211.

[23] M. Obeidi, E. McCarthy, B. O'Connell, I. Ul Ahad, and D. Brabazon, "Laser polishing of additive manufactured 316L stainless steel synthesized by selective laser melting," *Materials*, vol. 12, no. 6, p. 991, Mar. 2019, doi: 10.3390/ma12060991.

[24] B. Kang, G. Woo Kim, M. Yang, S.-H. Cho, and J.-K. Park, "A study on the effect of ultrasonic vibration in nanosecond laser machining," *Opt. Lasers Eng.*, vol. 50, no. 12, pp. 1817–1822, Dec. 2012, doi: 10.1016/j.optlaseng.2012.06.013.

[25] S. H. Alavi and S. P. Harimkar, "Melt expulsion during ultrasonic vibration-assisted laser surface processing of austenitic stainless steel," *Ultrasonics*, vol. 59, pp. 21–30, May 2015, doi: 10.1016/j.ultras.2015.01.013.

[26] H. P. Wang, Y. C. Guan, and H. Y. Zheng, "Smooth polishing of femtosecond laser induced craters on cemented carbide by ultrasonic vibration method," *Appl. Surf. Sci.*, vol. 426, pp. 399–405, Dec. 2017, doi: 10.1016/j.apsusc.2017.07.160.

[27] H. Wu, P. Zou, W. Yan, J. Cao, and K. F. Ehmann, "Micro wave patterns by vibrating-lens assisted laser machining," *J. Mater. Process. Technol.*, vol. 277, Mar. 2020, Art. no. 116424, doi: 10.1016/j.jmatprotec.2019.116424.

[28] H. Wu, P. Zou, J. Cao, and K. F. Ehmann, "Vibrating-lens-assisted laser drilling," *J. Manuf. Processes*, vol. 55, pp. 389–398, Jul. 2020, doi: 10.1016/j.jmapro.2020.03.005.

[29] J. R. Howell, R. Siegel, and M. P. Mengüç, "Energy transfer in plane layers and multidimensional geometries," in *Thermal Radiation Heat Transfer*, 5th ed. Boca Raton, FL, USA: CRC Press, 2010, pp. 535–559.

[30] J. Mazumder and W. M. Steen, "Heat transfer model for cw laser material processing," *J. Appl. Phys.*, vol. 51, no. 2, pp. 941–947, Feb. 1980, doi: 10.1063/1.327672.

[31] S. Yao, B. Chen, L. Dai, F. Zeng, J. Jin, and A. Abuliti, "Study on rapid measure of metallic material heat conductivity based on laser rapid heating," *J. Thermal Sci. Tech-Jpn.*, vol. 4, no. 1, pp. 87–90, Jan. 2005, doi: 10.1016/j.molcatb.2005.02.001.

[32] J. Xie, A. Kar, J. A. Rothenflue, and W. P. Latham, "Temperature-dependent absorptivity and cutting capability of CO_2, Nd: YAG and chemical oxygen–iodine lasers," *J. Laser Appl.*, vol. 9, no. 2, pp. 77–85, Apr. 1997, doi: 10.2351/1.4745447.
[33] J. Xie, A. Kar, J. A. Rothenflue, and W. P. Latham, "Comparative studies of metal cutting with high power lasers," *Proc. SPIE*, vol. 3092, pp. 764–767, Apr. 1997, doi: 10.1117/12.270183.
[34] S. Marimuthu, A. Triantaphyllou, M. Antar, D. Wimpenny, H. Morton, and M. Beard, "Laser polishing of selective laser melted components," *Int. J. Mach. Tools Manuf.*, vol. 95, pp. 97–104, Aug. 2015, doi: 10.1016/j.ijmachtools.2015.05.002.
[35] J. Zhao, Z. Liu, L. Chen, and Y. Hua, "Ultrasonic-induced phase redistribution and acoustic hardening for rotary ultrasonic roller burnished Ti-6Al-4 V," *Metall. Mater. Trans. A*, vol. 51, no. 3, pp. 1320–1333, Mar. 2020, doi: 10.1007/s11661-019-05594-2.
[36] R. C. V. Nostrand, "Design of experiments using the taguchi approach: 16 steps to product and process improvement," *Technometrics*, vol. 44, no. 3, p. 289, Aug. 2002, doi: 10.1198/004017002320256440.
[37] Z. Yuan, X. Chen, H. Zeng, K. Wang, and J. Qiu, "Identification of the elastic constant values for numerical simulation of high velocity impact on dyneema woven fabrics using orthogonal experiments," *Compos. Struct.*, vol. 204, pp. 178–191, Nov. 2018, doi: 10.1016/j.compstruct.2018.07.024.
[38] F. Zhou, J. Cheng, Y. Xu, S. Song, Y. Dai, and Q. Wang, "Investigation of orthogonal experiment for fabrication of a soldering joint for a 4-T HTS coil," *IEEE Trans. Appl. Supercond.*, vol. 24, no. 5, pp. 1–5, Oct. 2014, doi: 10.1109/TASC.2014.2331452.
[39] C. Chuanwen, S. Feng, L. Yuguo, and W. Shuyun, "Orthogonal analysis for perovskite structure microwave dielectric ceramic thin films fabricated by the RF magnetron-sputtering method," *J. Mater. Sci., Mater. Electron.*, vol. 21, no. 4, pp. 349–354, Jun. 2009, doi: 10.1007/s10854-009-9919-y.

DI KANG was born in Jinzhou, Liaoning, China, in 1988. He received the B.S. degree in mechanical engineering from Shenyang Aerospace University, Shenyang, China, in 2013, and the M.S. degree in mechanical engineering from Northeastern University at Shenyang, Shenyang, in 2018, where he is currently pursuing the Ph.D. degree in mechanical engineering. His research interests include the ultrasonic vibration-assisted laser polishing and ultrasonic vibration-assisted cutting composites.

PING ZOU was born in Shenyang, Liaoning, China, in 1963. He received the B.S. degree in mechanical engineering from the Jiangsu University of Science and Technology, Zhenjiang, China, in 1986, the M.S. degree in mechanical engineering from the Harbin Institute of Technology, Harbin, China, in 1989, and the Ph.D. degree in mechanical engineering from the Beijing University of Aeronautics and Astronautics, Beijing, China, in 1997. He is currently a Professor with the School of Mechanical Engineering and Automation, Northeastern University at Shenyang, Shenyang. His research interests include ultrasonic vibration-assisted machining, laser machining, parallel robots, and advanced cutting technology.

HAO WU was born in Yingkou, Liaoning, China, in 1990. He received the B.S. and Ph.D. degrees in mechanical engineering from Northeastern University at Shenyang, Shenyang, China, in 2013 and 2020, respectively. His research interests include ultrasonic vibration-assisted machining and laser machining.

WENJIE WANG was born in Huludao, Liaoning, China, in 1994. He received the B.S. and M.S. degrees in mechanical engineering from Northeastern University at Shenyang, Shenyang, China, in 2016 and 2018, respectively, where he is currently pursuing the Ph.D. degree in mechanical engineering. His research interests include the ultrasonic vibration-assisted laser machining and ultrasonic vibration-assisted cutting composites.

JILIN XU was born in Tai'an, Shandong, China, in 1990. He received the B.S. degree in mechanical engineering and automation from the University of Jinan, Jinan, China, in 2015, and the M.S. degree in mechanical engineering from Northeastern University at Shenyang, Shenyang, China, in 2019, where he is currently pursuing the Ph.D. degree in mechanical engineering. His research interest includes laser polishing.